

Structure prediction and activity analysis of human heme oxygenase-1 and its mutant

Zhen-Wei Xia, Wen-Pu Zhou, Wen-Jun Cui, Xue-Hong Zhang, Qing-Xiang Shen, Yun-Zhu Li, Shan-Chang Yu

Zhen-Wei Xia, Yun-Zhu Li, Shan-Chang Yu, Department of Pediatrics, Rui Jin Hospital, Shanghai Second Medical University, Shanghai 200025, China

Wen-Pu Zhou, Wen-Jun Cui, Xue-Hong Zhang, College of Life Science and Biotechnology, Shanghai Jiaotong University & Chinese Academy of Sciences, Shanghai Branch, Shanghai 200030, China

Qing-Xiang Shen, Shanghai Institute of Planned Parenthood Research, Shanghai 200032, China

Supported by the National Natural Science Foundation of China, No. 30170988, Shanghai Municipal Education Commission Foundation, No.2000B06, and Shanghai Jiaotong University-Shanghai Second Medical University Cooperative Foundation

Correspondence to: Dr. Xia Zhen Wei, Department of Pediatrics, Rui Jin Hospital, Shanghai Second Medical University, 197 Rui Jin Er Road, Shanghai 200025, China. xzw63@hotmail.com

Telephone: +86-21-64333414 **Fax:** +86-21-64333414

Received: 2004-01-02 **Accepted:** 2004-02-03

Abstract

AIM: To predict wild human heme oxygenase-1 (whHO-1) and hHO-1 His25Ala mutant (Δ hHO-1) structures, to clone and express them and analyze their activities.

METHODS: Swiss-PdbViewer and Antheptrot 5.0 were used for the prediction of structure diversity and physical-chemical changes between wild and mutant hHO-1. hHO-1 His25Ala mutant cDNA was constructed by site-directed mutagenesis in two plasmids of *E. coli* DH5 α . Expression products were purified by ammonium sulphate precipitation and Q-Sepharose Fast Flow column chromatography, and their activities were measured.

RESULTS: rHO-1 had the structure of a helical fold with the heme sandwiched between heme-heme oxygenase-1 helices. Bond angle, dihedral angle and chemical bond in the active pocket changed after Ala25 was replaced by His25, but Ala25 was still contacting the surface and the electrostatic potential of the active pocket was negative. The mutated enzyme kept binding activity to heme. Two vectors pBHO-1 and pBHO-1(M) were constructed and expressed. Ammonium sulphate precipitation and column chromatography yielded 3.6-fold and 30-fold higher purities of whHO-1, respectively. The activity of Δ hHO-1 was reduced 91.21% after mutation compared with whHO-1.

CONCLUSION: Proximal His25 ligand is crucial for normal hHO-1 catalytic activity. Δ hHO-1 is deactivated by mutation but keeps the same binding site as whHO-1. Δ hHO-1 might be a potential inhibitor of whHO-1 for preventing neonatal hyperbilirubinemia.

Xia ZW, Zhou WP, Cui WJ, Zhang XH, Shen QX, Li YZ, Yu SC. Structure prediction and activity analysis of human heme oxygenase-1 and its mutant. *World J Gastroenterol* 2004; 10(16): 2352-2356

<http://www.wjgnet.com/1007-9327/10/2352.asp>

INTRODUCTION

Heme oxygenase (HO) is responsible for the physiological breakdown of heme into equimolar amounts of biliverdin, carbon monoxide, and iron. Three isoforms (HO-1, HO-2, and HO-3) have been identified. HO-1 is ubiquitous, its mRNA levels and activity can be increased several-fold by heme, other metalloporphyrins, transition metals, and stress-inducing stimuli. In contrast, HO-2 is present chiefly in brain and testes and is virtually uninducible. HO-3 has very low activity; its physiological functions probably include heme binding. The HO system has been strongly highlighted for its potential significance in maintaining cellular homeostasis. Nevertheless the physiological correlations of the three isoforms and their reciprocal interrelation have been poorly understood^[1-4].

HO-1 regulates the levels of serum bilirubin as the rate-limiting enzyme in heme degradation pathway. Recent reports showed that HO-1 was identified as an ubiquitous stress protein and it had important physiological roles. Overexpression of HO-1 gene resulted in protection from cytokine-induced oxidative stress^[5], inflammation^[6-9], apoptosis^[10-17] and proliferation^[18-25].

It has been reported that histidine (His) residues at positions 25, 84, 119 and 132 in HO-1 sequence are conserved in rat, human, mouse and chicken. These histidines may be important for heme-binding^[26]. His25 and His132 mutants were reported for the proximal heme iron ligand in rat heme oxygenase-1 (rHO-1)^[27]. The unambiguous spectroscopic demonstration that His25 is the proximal iron ligand leaves the role of His132 uncertain. His 25 is essential for heme degradation activity of the enzyme. The research on human HO-1 (hHO-1) structure has been shown that hHO-1 embodies a novel protein fold that consists primarily of α -helices, and the heme is held between two of these helices^[28].

It is unclear whether hHO-1 mutant has the same characteristics and displays catalytic inactivity but binding heme as Ala replacing His 25. In this study, the characteristics of wild hHO-1 (whHO-1) and its mutant were predicted by bioinformatics method. On the basis of the results, the truncated hHO-1 cDNA mutant was constructed by site-directed mutagenesis. Two expression plasmids, pBHO-1 and pBHO-1 (M) containing whHO-1 and hHO-1 His25Ala mutant (Δ hHO-1), respectively, were constructed and expressed in *E. coli*, and then isolated, purified and analyzed of their activities analysis.

MATERIALS AND METHODS

Materials

Swiss-PdbViewer and Antheptrot 5.0 were from GlaxoSmithKline R&D and the Swiss Institute of Bioinformatics and CBI, BeiJin University respectively. Plasmid pBHO-1 was provided by Lightning and Ortiz de Montellano (Department of Pharmaceutical Chemistry, University of California). Mutation primer was synthesized by Boya Company. Anti-HO-1 antibody, RNase and DNase were purchased from Sigma. Restriction endonucleases were from Haojia Company, Q-Sepharose Fast Flow Anion exchange column was from Amersham Pharmacia. pBS II KS⁺/-, pGEM3Z and *E. coli* strain DH5 α were stored in author's laboratory.

Methods

Structure analysis of hHO-1 and its mutant Swiss-PdbViewer and Antheprot 5.0 were used to analyze the structure diversity and physical-chemical changes between whHO-1 and Δ hHO-1. Then the prime structure was refined by energy minimization. Gromos96 was used as force field. The molecular surfaces and electrostatic potential were calculated. The rationality of the resulted model was validated by Ramachandran plot.

Construction of Δ hHO-1 expression vector pBHO-1 (M) *EcoRI/SalI* digested fragment of pBHO-1, which is from expression vector containing the truncated hHO-1 cDNA (804 bp), was cloned into the *EcoRI/SalI* sites of plasmid pBSKS II to construct plasmid pBSHO-1. hHO-1 His25Ala mutant cDNA could be amplified by PCR using pBSHO-1 as template. The mutation primer (5'-GACAGCATGCCCCAGGATTTGTCAGAGGCCCTGAAGGAGGCCACCAAGGAGGTGGCCACCC-3') and reverse primer (5'-AACAGCTATGACCATG-3') were chosen, which have changed the His 25 codon CAC into Ala codon GCC. The reaction conditions were: at 94 °C for 5 min, followed by 94 °C for 1 min, at 55 °C for 1 min, 72 °C for 2 min, with amplification repeated for 30 cycles, and finally at 72 °C for 10 min. The mutant cDNA was gel-purified and digested with *SphI/SalI* and then cloned into *SphI/SalI* sites of plasmid pGEM3Z. hHO-1 His25Ala mutant cDNA was screened by restriction digestion and confirmed by sequencing in pGEM3ZHO-1(M). Verified hHO-1 mutant cDNA was obtained from *SphI/SalI* digested fragment of pGEM3ZHO-1 (M) and then cloned into pBHO-1, thus the expression vector containing Δ hHO-1 was designated as pBHO-1 (M) (Figure 1).

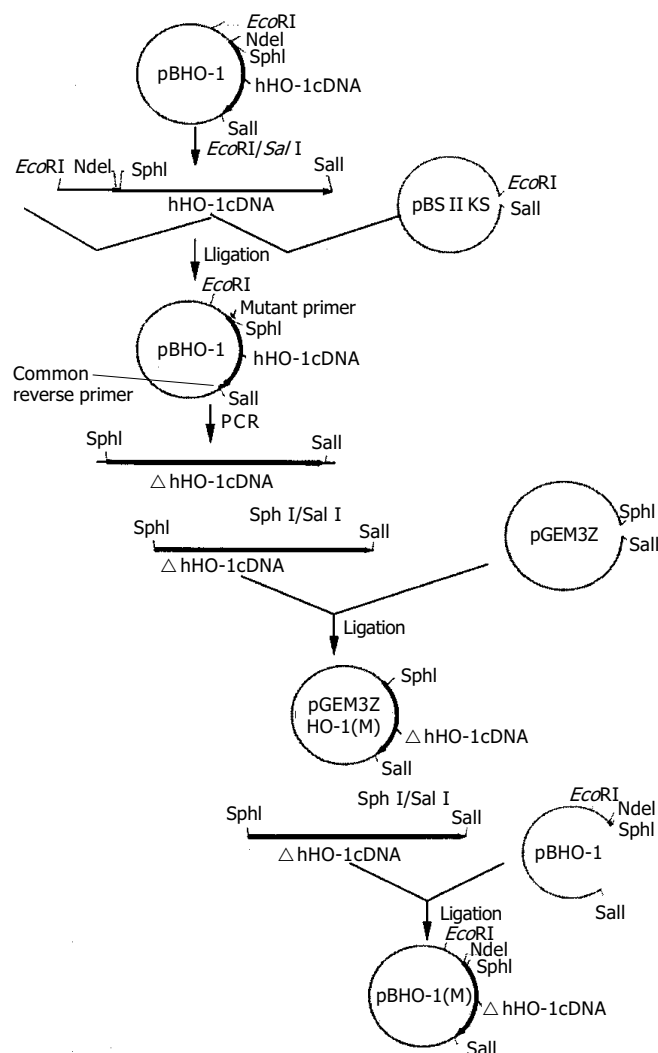


Figure 1 Construction of expression vector pBHO-1(M).

Expression and purification of whHO-1 and Δ hHO-1 A total of 5.0 mL inoculum was set up from plates with fresh colonies of transformed *E. coli* DH5 α and incubated at 37 °C for 12-16 h. From the fresh cultures 400 μ L was used to inoculate into 40 mL cultures of the same media. The cells were grown at 37 °C until A_{600} reached 0.3-0.5, then added with 0.5 mmol/L IPTG for 18 h. The expression products were harvested and analyzed with sodium dodecyl sulfate-polyacrylamide gel (SDS-PAGE) and Western blotting at the time points of 7, 9 and 11 h, respectively, after addition of IPTG. Then 500 mL inoculum in medium was incubated under same condition. The harvested cells were centrifuged at 6 000 r/min for 20 min at 4 °C, washed once in PBS, and then centrifuged at 6 000 r/min for 10 min at 4 °C. The cells were lysed in 50 mmol/L Tris buffer (pH 8.0) containing 1 mmol/L dithiothreitol, 1 mmol/L EDTA, 1 mmol/L phenylmethanesulfonyl fluoride (PMSF) and sonicated for 10 min. Then the cells were centrifuged at 13 000 r/min for 1 h at 4 °C. The supernatant was collected and ammonium sulfate was added to a final concentration of 30%, and the solution was stirred for 60 min. Following centrifugation (13 000 r/min for 20 min), ammonium sulfate concentration was raised to 60% of saturation. The pellets precipitated by ammonium sulfate were collected and resuspended in 0.1 mol/L potassium phosphate (pH 7.4) and then dialyzed against 1 g/L NH_4HCO_3 for 4 h ($\times 4$ -times). Protein 130 mg was applied to a Q-Sepharose Fast Flow anion column and eluted with a step gradient of 50 mmol/L Tris-HCl (pH 7.4) (buffer A) containing 0-0.5 mol/L NaCl (buffer B). The fractions containing hHO-1 protein were pooled together and applied to Q-Sepharose Fast Flow anion column again. The protein was eluted with a step gradient of 50 mmol/L Tris-HCl (pH 8.4) (buffer C) containing 0-0.5 mol/L NaCl (buffer B). The gradient was increased linearly from 0-100% buffer B. Fractions containing hHO-1 protein were pooled and dialyzed against 1 g/L NH_4HCO_3 for 4 h ($\times 4$ -times).

Western blotting Blot analysis was carried out as previously described^[29]. Microsomal protein samples were fractionated by SDS-PAGE under denaturing conditions. The separated proteins were electrophoretically transferred to a nitrocellulose membrane. Western blotting was carried out using monoclonal antibody to hHO-1 and the immunoreactive bands were visualized by staining (1 mol/L Tris-HCl pH 9.5, 1 mol/L MgCl_2 , 0.1 mg/mL nitro-blue tetrazolium, 0.1 mg/mL 5-bromo-4-chloro-3-indolylphosphate-toluidine salt).

Analysis of whHO-1 and Δ hHO-1 activities Protein samples were incubated with heme (50 μ mol/L), rat liver cytosol (5 mg/mL), MgCl_2 (2 mmol/L), glucose-6-phosphate dehydrogenase (1 unit), glucose-6-phosphate (2 mmol/L), and NADPH (0.8 mmol/L) in 0.5 mL of 0.1 mol/L potassium phosphate buffer (pH 7.4), for 60 min at 37 °C. Reaction was stopped by putting the tubes on ice, and reaction solution was extracted with chloroform. The rate of bilirubin formation was monitored at 464 nm by a spectrophotometer and then calculated using an extinction coefficient of 40.0 $\text{mmol}/(\text{L}\cdot\text{cm})$ ^[29].

RESULTS

Whole structure comparison between whHO-1 and Δ hHO-1

In heme-heme oxygenase-1 complex, heme is sandwiched in whHO-1. When Ala 25 replaces His 25, the complex structure does not change. In the heme-binding pocket, Ala 25 loses contacting with heme as His 25 does. The molecular surface has a catalytic reaction pocket, which includes Thr 21, His 25, Ala 28, Glu 29, Gly 139, Asp140, Gly 143. After binding heme, His 25 still lies on the surface but Gly139, Asp140 and Gly143 are covered by heme. When Ala 25 replaces His 25, Ala 25 still lies in the surface (Figure 2). In activity domain, the bond angle, dihedral angle and chemical bond appear differently after Ala 25 replacing His 25 (Table 1, Figure 3).

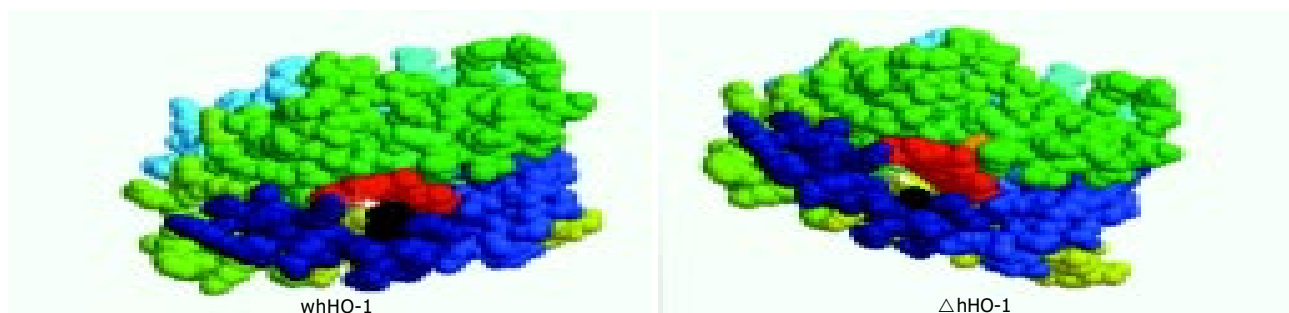


Figure 2 Prime simulated structure of whHO-1 and Δ hHO-1. Red: heme; Black: His 25 and Ala 25. Ala 25 loses contacting with heme as His 25 does in the heme-binding pocket.



Figure 3 Changes of bond angle, dihedral angle and chemical bond.



Figure 4 Molecular surfaces and electrostatic potential of whHO-1 and Δ hHO-1. The electrostatic potential of active pocket is -1.800 .

Table 1 Bond angle, dihedral angle and the distance between atoms of Δ hHO-1

		Prime simulation	Optimized simulation
Bond angle	C24-N-CA	119.12	121.79
	CA-C-N26	115.92	115.12
Distance between atoms	CB-FE	5.55	5.58
	CA-FE	6.28	6.26
Dihedral angle	ω	175.40	175.61
	ϕ	-40.78	-34.45
	ψ	-60.70	-62.89

Though Ala 25 replaces His 25, the molecular surfaces and electrostatic potential changed little (Figure 4). The electrostatic potential of active pocket was still negative. The mutagenesis had no apparent effect on molecular surface. Ramachandran plot showed that dihedral angles ϕ (-33.98) and ψ (-64.46) were in rational range.

Antheprot 5.0 analysis also showed that there was no alteration in the secondary structure between whHO-1 and Δ hHO-1. Garnier, Gibrat, DPM and homology predicted the same results. Physical-chemical characteristics showed somewhat alteration. Hydrophobicity increased, while hydrophilicity decreased. There was no change in antigenicity, helical membranous regions and solvent accessibility.

Construction of pBHO-1(M) containing Δ hHO-1

hHO-1 cDNA was site mutated at His 25 (to Ala) by PCR with pBSHO-1 as the template. The 866-bp PCR product showed that nucleotide 3-773 sequences encoded hHO-1 domain from 25-265 AA. The mutant cDNA was cloned into the *SphI/SalI* sites of plasmid pGEM3Z for constructing plasmid pGEM3ZHO-1 (M). hHO-1 His25Ala mutant cDNA was confirmed by sequencing in pGEM3ZHO-1 (M). The verified hHO-1 mutant cDNA from the *SphI/SalI* digested fragment of pGEM3ZHO-1 (M) was cloned into pBHO-1, thus the expression vector containing Δ hHO-1 was designated as pBHO-1 (M) (Figure 1). Both whHO-1 and Δ hHO-1 cDNAs equally encoded the proteins containing 265 amino acids with a M_r 30 500.

Expression and identification of whHO-1 and Δ hHO-1 in *E. coli* DH5 α

E. coli DH5 α was transformed by pBHO-1 and pBHO-1 (M), respectively, and treated with 0.5 mmol/L IPTG for 18 h at 37 °C. Equal quantities of cells transformed with different expression vectors were lysed by protein electrophoresis buffer. Untransformed *E. coli* sample was used as the negative control. As shown in Figure 5, *E. coli* DH5 α transformed pBHO-1 or pBHO-1 (M) highly expressed whHO-1 and Δ hHO-1 with a M_r 30 500. Meanwhile, *E. coli* DH5 α not treated with IPTG also expressed whHO-1 and Δ hHO-1, but its expression yield

was significantly lower than that of transformed cells. Analysis of cell lysates showed that whHO-1 and Δ hHO-1 were mainly present in the supernatants.

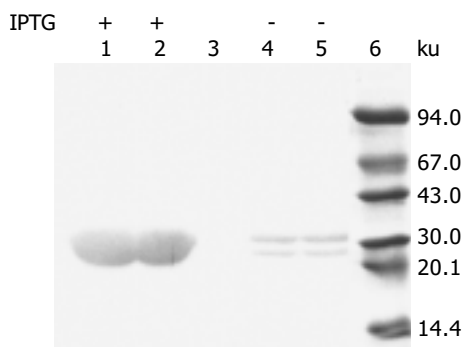


Figure 5 Western blotting of whHO-1 and Δ hHO-1 expressed in DH5 α . Lanes 1, 2: Expression products of pBHO-1 and pBHO-1(M) in DH5 α induced with IPTG; lane 3: Control; lanes 4, 5: Expression products of pBHO-1 and pBHO-1(M) in DH5 α not treated with IPTG; lane 6: Marker.

Purification of whHO-1 and Δ hHO-1

The protein with a M_r 30 500 was purified by 30-60% ammonium sulphate precipitation and analyzed by SDS-PAGE.

After precipitated with ammonium sulphate, whHO-1 sample was applied to Q-Sepharose Fast Flow anion column (pH 7.4). The first peak containing whHO-1 (No. 1-3 tubes) was collected (Figure 6A) and loaded on Q-Sepharose Fast Flow anion column (pH 8.4) again. whHO-1 was shown to be eluted in the second peak (No. 49-63 tubes) (Figure 6B). All samples were analyzed by SDS-PAGE and Western blotting in order to identify the separation efficiency. The activity of whHO-1 after purification was 30-fold higher than that in the initial lysates (Table 2).

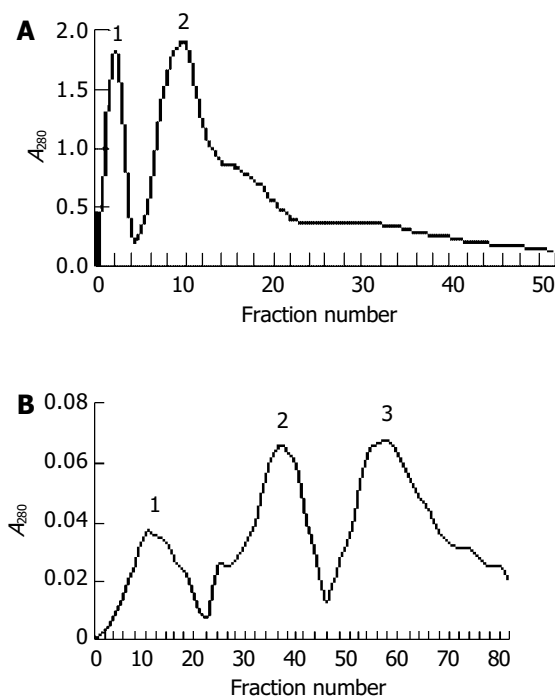


Figure 6 Q-Sepharose Fast Flow column chromatography. A: pH 7.4 buffer; B: pH 8.4 buffer.

Precipitated Δ hHO-1 was further purified in the same way as described above. One purified protein's M_r was 30 500. The purified whHO-1 and Δ hHO-1 are shown on SDS-PAGE (Figure 7).

Table 2 whHO-1 activities after different purification

	Supernatant of DH5 α lysates	30-60% (NH ₄) ₂ SO ₄	Q-Sepharose fast flow
whHO-1 activity (U·mg ⁻¹ ·h ⁻¹)	0.5	1.8	15
Purification fold	1.0	3.6	30

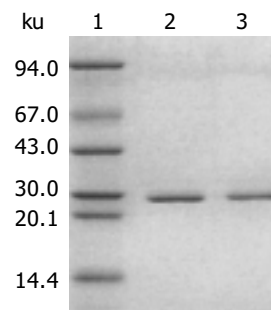


Figure 7 SDS-PAGE analysis of purified whHO-1 and Δ hHO-1. Lane 1: Marker; lane 2: whHO-1; lane 3: Δ hHO-1.

DISCUSSION

An understanding of the structure and function of hHO-1 is of importance in the context of human diseases, but due to limited accessibility and difficulties associated with their purification from microsomal membranes, little direct information has been available until the expression of rHO-1 in *E. coli* was achieved. The protein thus obtained is soluble, easily purified, and fully active. Encouraged by this result, the research on HO-1 including hHO-1 has been thriving.

hHO-1 is anchored to the endoplasmic reticulum membrane via a stretch of hydrophobic residues at the C-terminus. While full-length hHO-1 consists of 288 residues, a truncated version with residues 1-265 has been expressed as a soluble active enzyme in *E. coli*. This recombinant enzyme precipitated from ammonium sulfate solution but without a high purity for studies^[30].

In the present studies, we acquired the structures of hHO-1 with residues 1-265 and its mutant using Swiss-PdbViewer. Due to the high similarity between hHO-1 and its mutant, the hHO-1 structure was used as template. Through homology modeling, template selection and target-template alignment, a molecular backbone and side chains were built in one step. Results demonstrated that the refined model, as well as the entire assay, was valid. Predictions of the structure showed that hHO-1 and its mutant had similar electrostatic potential suggesting that they have similar affinity to heme in electrostatic potential. Ala is a hydrophobic amino acid without chemical activity, and its side chain is short. So it has no interference with binding through steric hindrance.

Rat His25Ala HO-1 provides a new approach to construct hHO-1 mutant. hHO-1 mutants were prepared in which residue His25 was replaced by Ala using site-directed mutagenesis to understand the role of hHO-1 His25 in keeping the activity of this enzyme. In this study, the synthesized forward primer was applied in which His25 codon was replaced by the Ala codon. This cDNA was cloned into the expression vector pBHO-1, then pBHO-1 and pBHO-1(M) were transformed into *E. coli*, which were used to express whHO-1 and Δ hHO-1. Although the endogenous protein expression of *E. coli* could disturb the measurement of whHO-1 and its mutants by SDS-PAGE, hHO-1 and its mutant expression could be detected by anti-HO-1 antibody in Western blotting.

Our study shows that precipitation with ammonium sulfate can enrich whHO-1 and Δ hHO-1 in the lysates. Compared with the whHO-1 activity, Δ hHO-1 activity was reduced by

91.21%. It suggests that His25 is crucial for the catalytic activity of hHO-1, the proximal His25 ligand is critically required for normal hHO-1 catalysis. The results are similar to previous reports^[31-35].

hHO-1 has anti-inflammatory^[6-9], antiapoptotic^[10-17], and antiproliferative^[18-25] effects, and salutary effects on neonatal hyperbilirubinemia^[36]. The results show a valid way to control the concentration of bilirubin in human, since hHO-1 is the rate-limiting enzyme in the catabolic reaction of heme, which ultimately produces bilirubin in human body. High-level bilirubin in newborns, patients with the Crigler-Najjar type I syndrome and certain hepatic disorders can result in hyperbilirubinemia, especially in patients whose bilirubin is impaired for developmental or genetic reasons. Currently clinical methods are only to eliminate formed bilirubin. There is no effective way to inhibit bilirubin production, and Δ hHO-1 would be a potential inhibitor for bilirubin production.

REFERENCES

- 1 Elbirt KK, Bonkovsky HL. Heme oxygenase: recent advances in understanding its regulation and role. *Proc Assoc Am Physicians* 1999; **111**: 438-447
- 2 Scapagnini G, D'Agata V, Calabrese V, Pascale A, Colombrita C, Alkon D, Cavallaro S. Gene expression profiles of heme oxygenase isoforms in the rat brain. *Brain Res* 2002; **954**: 51-59
- 3 Montellano PR. The mechanism of heme oxygenase. *Curr Opin Chem Biol* 2000; **4**: 221-227
- 4 Chu GC, Katakura K, Zhang X, Yoshida T, Ikeda-Saito M. Heme degradation as catalyzed by a recombinant bacterial heme oxygenase (Hmu O) from *Corynebacterium diphtheriae*. *J Biol Chem* 1999; **274**: 21319-21325
- 5 Immenschuh S, Ramadori G. Gene regulation of heme oxygenase-1 as a therapeutic target. *Biochem Pharmacol* 2000; **60**: 1121-1128
- 6 Kushida T, Li Volti G, Quan S, Goodman A, Abraham NG. Role of human heme oxygenase-1 in attenuating TNF-alpha-mediated inflammation injury in endothelial cells. *J Cell Biochem* 2002; **87**: 377-385
- 7 Alcaraz MJ, Fernandez P, Guillen MI. Anti-inflammatory actions of the heme oxygenase-1 pathway. *Curr Pharm Des* 2003; **9**: 2541-2551
- 8 Wagener FA, van Beurden HE, von den Hoff JW, Adema GJ, Figdor CG. The heme-heme oxygenase system: a molecular switch in wound healing. *Blood* 2003; **102**: 521-528
- 9 Chok Mk, Senechal M, Dorent R, Mallat Z, Leprince P, Bonnet N, Pavie A, Ghossoub JJ, Gandjbakhch I. Apoptosis and expression of heme oxygenase-1 in heart transplant recipients during acute rejection episodes. *Transplant Proc* 2002; **34**: 3239-3240
- 10 Rothfuss A, Speit G. Overexpression of heme oxygenase-1 (HO-1) in V79 cells results in increased resistance to hyperbaric oxygen (HBO)-induced DNA damage. *Environ Mol Mutagen* 2002; **40**: 258-265
- 11 Takata K, Kitamura Y, Kakimura J, Shibagaki K, Taniguchi T, Gebicke-Haerter PJ, Smith MA, Perry G, Shimohama S. Possible protective mechanisms of heme oxygenase-1 in the brain. *Ann N Y Acad Sci* 2002; **977**: 501-506
- 12 Katori M, Busuttill RW, Kupiec-Weglinski JW. Heme oxygenase-1 system in organ transplantation. *Transplantation* 2002; **74**: 905-912
- 13 Cornelussen RN, Knowlton AA. Heme-oxygenase-1: versatile sentinel against injury. *J Mol Cell Cardiol* 2002; **34**: 1297-1300
- 14 Ke B, Shen XD, Zhai Y, Gao F, Busuttill RW, Volk HD, Kupiec-Weglinski JW. Heme oxygenase 1 mediates the immunomodulatory and antiapoptotic effects of interleukin 13 gene therapy *in vivo* and *in vitro*. *Hum Gene Ther* 2002; **13**: 1845-1857
- 15 Abraham NG, Kushida T, McClung J, Weiss M, Quan S, Lafaro R, Darzynkiewicz Z, Wolin M. Heme oxygenase-1 attenuates glucose-mediated cell growth arrest and apoptosis in human microvessel endothelial cells. *Circ Res* 2003; **93**: 507-514
- 16 Colombrita C, Lombardo G, Scapagnini G, Abraham NG. Heme oxygenase-1 expression levels are cell cycle dependent. *Biochem Biophys Res Commun* 2003; **308**: 1001-1008
- 17 Pandya HC, Snetkov VA, Twort CH, Ward JP, Hirst SJ. Oxygen regulates mitogen-stimulated proliferation of fetal human airway smooth muscle cells. *Am J Physiol Lung Cell Mol Physiol* 2002; **283**: L1220-1230
- 18 Perrella MA, Yet SF. Role of heme oxygenase-1 in cardiovascular function. *Curr Pharm Des* 2003; **9**: 2479-2487
- 19 Morse D. The role of heme oxygenase-1 in pulmonary fibrosis. *Am J Respir Cell Mol Biol* 2003; **29**(3 Suppl): S82-86
- 20 Stanford SJ, Walters MJ, Hislop AA, Haworth SG, Evans TW, Mann BE, Motterlini R, Mitchell JA. Heme oxygenase is expressed in human pulmonary artery smooth muscle where carbon monoxide has an anti-proliferative role. *Eur J Pharmacol* 2003; **473**: 135-141
- 21 Li L, Grenard P, Nhieu JT, Julien B, Mallat A, Habib A, Lotersztajn S. Heme oxygenase-1 is an antifibrogenic protein in human hepatic myofibroblasts. *Gastroenterology* 2003; **125**: 460-469
- 22 Bauer I, Rensing H, Florax A, Ulrich C, Pistorius G, Redl H, Bauer M. Expression pattern and regulation of heme oxygenase-1/heat shock protein 32 in human liver cells. *Shock* 2003; **20**: 116-122
- 23 Hancock WW, Buelow R, Sayegh MH, Turka LA. Antibody-induced transplant arteriosclerosis is prevented by graft expression of anti-oxidant and anti-apoptotic genes. *Nat Med* 1998; **4**: 1392-1396
- 24 Zhang M, Zhang BH, Chen L, An W. Overexpression of heme oxygenase-1 protects smooth muscle cells against oxidative injury and inhibits cell proliferation. *Cell Res* 2002; **12**: 123-132
- 25 Soares MP, Lin Y, Anrather J, Cszizmadia E, Takigami K, Sato K, Grey ST, Colvin RB, Choi AM, Poss KD, Bach FH. Expression of heme oxygenase-1 can determine cardiac xenograft survival. *Nat Med* 1998; **4**: 1073-1077
- 26 Liu Y, Moenne-Loccoz P, Hildebrand DP, Wilks A, Loehr TM, Mauk AG, Ortiz de Montellano PR. Replacement of the proximal histidine iron ligand by a cysteine or tyrosine converts heme oxygenase to an oxidase. *Biochemistry* 1999; **38**: 3733-3743
- 27 Ito-Maki M, Ishikawa K, Matera KM, Sato M, Ikeda-Saito M, Yoshida T. Demonstration that histidine 25, but not 132, is the axial heme ligand in rat heme oxygenase-1. *Arch Biochem Biophys* 1995; **317**: 253-258
- 28 Schuller DJ, Wilks A, Ortiz de Montellano PR, Poulos TL. Crystal structure of human heme oxygenase-1. *Nat Struct Biol* 1999; **6**: 860-867
- 29 Xia Z, Shao J, Shen Q, Wang J, Li Y, Chen S, Yu S. The preparation of rat heme oxygenase-1 mutant to reduce the level of bilirubin. *Chin Med J* 2001; **114**: 348-351
- 30 Schuller DJ, Wilks A, Ortiz de Montellano P, Poulos TL. Crystallization of recombinant human heme oxygenase-1. *Protein Sci* 1998; **7**: 1836-1838
- 31 Auclair K, Moenne-Loccoz P, Ortiz de Montellano PR. Roles of the proximal heme thiolate ligand in cytochrome p450 (cam). *J Am Chem Soc* 2001; **123**: 4877-4885
- 32 Wilk A, Medzihradsky KF, Ortiz de Montellano PR. Heme oxygenase active-site residues identified by heme-protein cross-linking during reduction of CBrC13. *Biochemistry* 1998; **37**: 2889-2896
- 33 Lad L, Schuller DJ, Shimizu H, Friedman J, Li H, Ortiz de Montellano PR, Poulos TL. Comparison of the heme-free and -bound crystal structures of human heme oxygenase-1. *J Biol Chem* 2003; **278**: 7834-7843
- 34 Foresti R, Motterlini R. The heme oxygenase pathway and its interaction with nitric oxide in the control of cellular homeostasis. *Free Radic Res* 1999; **31**: 459-475
- 35 Chang SH, Barbosa-Tessmann I, Chen C, Kilberg MS, Agarwal A. Glucose deprivation induces heme oxygenase-1 gene expression by a pathway independent of the unfolded protein response. *J Biol Chem* 2002; **277**: 1933-1940
- 36 Maines MD. The heme oxygenase system: a regulator of second messenger gases. *Annu Rev Pharmacol Toxicol* 1997; **37**: 517-554